Rapid Thickness Reading of $CH_3NH_3PbI_3$ Thin Films from Color Maps

Massimo Spina, Claudio Grimaldi, Bálint Náfrádi, László Forró and Endre Horváth*

Laboratory of Physics of Complex Matter (LPMC), Ecole Polytechnique Fédérale de Lausanne, 1015 Lausanne, Switzerland

Abstract

Hybrid halide perovskite photovoltaic materials show a remarkable light conversion efficiency in various optoelectronic devices. In the fabrication of these solar cells, light emitting diodes, laser and photodetector prototypes the thickness of the perovskite is an important parameter since the light is absorbed in the top few hundred nanometers of the material. Nevertheless, making perovskite coatings with various solution-based and evaporation methods showing highly reproducible thickness and area coverage is still an issue. Therefore, rapid and reliable quality-control of the film morphology is needed. This report shows a simple, rapid, and calibration-free method for reading the thickness directly from the color map of nanowire perovskite films seen in standard optical microscope with visible light.

1 Introduction

The astonishingly fast increase during the last few years of light conversion efficiency in organometal halide perovskite solar cells has made this class of materials very promising for low-cost and high-efficiency photovoltaics.[1,2,3,4,5,6] Nowadays, the record photovoltaic efficiency is held by methylammonium lead iodide $CH_3NH_3PbBr_3$ blended with

formamidinium lead iodide that shows a remarkable conversion efficiency of about 20 %.[7] Furthermore, it has been realized that the organo-metal halide perovskites may also prove highly useful for making efficient lasers,[8,9] very bright light-emitting diodes,[10] and miniaturized photo-detectors in hybrid devices.[11]

The crystallite size and geometry are important factors also in consideration of the fact that they greatly influence the physico-chemical properties of the material. In particular, the perovskite height (or thickness) is a crucial parameter in photovoltaics and other optoelectronic devices. However, optimization of the layer thickness is hindered by the incomplete understanding of the crystallization mechanism in diverse deposition methods and the lack of a rapid quality-control of the film morphology. A reliable and quick method for identifying the film thickness and surface coverage may help to overcome this issue. In this respect, optical imaging is an easy, rapid and nondestructive technique which does not rely on expensive and sophisticated characterization tools as in, e.g., ellipsometry or laser scanning confocal measurements. Under suitable calibration conditions, techniques based on optical imaging have already used for the characterization of thin films,[12,13] and two-dimensional materials like, e.g., graphene,[14,15,16,17] and transition metal dichalcogenides.[18,19]

In this article, we introduce a new optical method that allows to automatically reconstruct the thickness of discontinuous or continuous films of $CH_3NH_3PbI_3$ (abbreviated as $MAPbI_3$) nanowires[20,21] slip-coated on SiO_2/Si and TiO_2/Si substrates, directly from the optical images of the multilayer system. Unlike other optical techniques based on optical contrast[14,15,18,19] and color difference[16,17] methods, our approach does not make use of any calibration from, e.g., atomic force microscopy (AFM) or Raman measurements. The use of nanowires enables us to extract a great range of thicknesses that correspond to those measured by AFM, and for a variety of nanowire deposition conditions. We show that the presented technique enables

rapid and calibration-free thickness reading also of large-scale optical images, leading to clear advantages over other more sophisticated and expensive characterization tools.

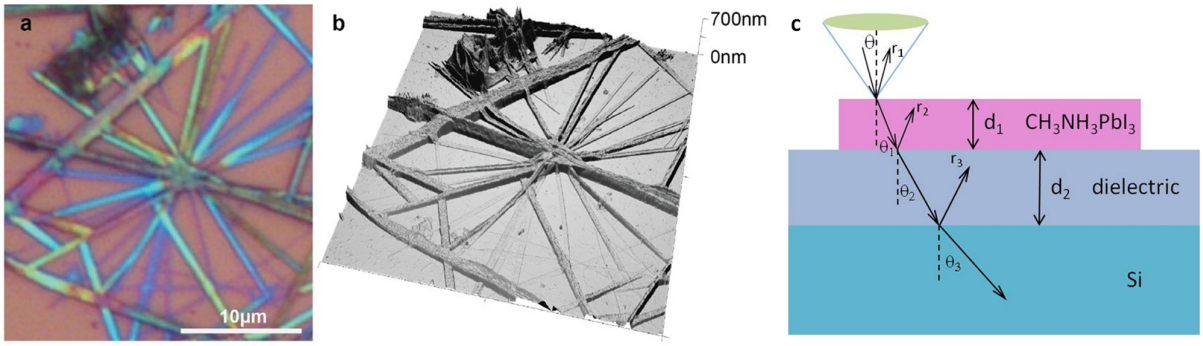

Figure 1. (a) Optical image of a bunch of nanowires slip-coated on a 280 nm thick SiO_2 layer (a). Three-dimensional AFM image reconstruction of the imaged set of nanowires. We can see from the AFM micrograph that different colors correspond to different nanowire thicknesses. (c) Schematic representation of optical transmission and reflection for a flat perovskite film of thickness d_1 deposited on a dielectric layer of thickness d_2 grown on top of a Si substrate.

2 Synthesis and characterization

$MAPbI_3$ nanowires were synthesized from a saturated solution of $MAPbI_3$, obtained by dissolving small single crystals in dimethylformamide. The solution was dropped onto a glass microscope slide and covered with a second glass slide so that the excess solution squeezed out; the rest forming a homogenous liquid film between the glass plates.[20] The excess of the $MAPbI_3$ solution was removed from the sides by soaking with a tissue. Next, the bottom substrate was held in place while gradually sliding the upper glass plate, exposing the thin liquid film to air and inducing solvent evaporation. Further details of the synthesis can be found in Ref. (20).

Optical microscopy was performed with a Nikon Optiphot 200 microscope (50x, numerical aperture= 0.8) equipped with high-intensity halogen lamp. The thickness of $MAPbI_3$ nanowires was measured with a Bruker Dimension FastScan atomic force microscope in tapping mode.

3 Results and Discussion

3.1 Calculation of color components

$MAPbI_3$ nanowires can have different morphologies and dimensions according to the parameters involved in the synthesis process (solvent concentration, temperature, sliding speed, etc.). The slip-coated nanowires can have rectangular or hollow cross section and thickness ranging between few to hundreds of nanometers, as seen in the three-dimensional AFM reconstruction images shown in Figure 1b. Using a silicon substrate coated with a dielectric layer (e.g. SiO_2, TiO_2) the difference in height between the nanowires corresponds to a different color contrast in the optical images taken under white light illumination. Figure 1a shows slip-coated perovskite nanowires possessing a variety of colors according to their thickness and the dielectric layer.

The different colors shown in Figure 1a and their dependence upon the material thickness can be understood and reproduced by standard thin film optics theory. To this end, we follow Ref.(22) which describes a procedure to calculate the dependence of the red, green, blue (RGB) parameters on the thicknesses and optical properties of multilayer systems. We express the reflectance of the multilayer system $MAPbI_3$/dielectric/Si as follows:[14,16,23]

$$R(\lambda) = \left| \frac{r_1 + r_2 e^{-2i\delta_1} + r_3 e^{-2i(\delta_1+\delta_2)} + r_1 r_2 r_3 e^{-2i\delta_2}}{1 + r_1 r_2 e^{-2i\delta_1} + r_1 r_3 e^{-2i(\delta_1+\delta_2)} + r_2 r_3 e^{-2i\delta_2}} \right|^2 \quad (1)$$

where λ is the wavelength of the incident light, r_1, r_2, and r_3 are the amplitudes of the light reflected at air/$MAPbI_3$, $MAPbI_3$/dielectric, and dielectric/silicon interfaces, respectively. In

equation 1, $\delta_1 = (2\pi d_1 / \lambda)(n_1 - ik_1)\cos\theta_1$ and $\delta_2 = (2\pi d_2 / \lambda)(n_2 - ik_2)\cos\theta_2$ are the phase changes across $MAPbI_3$ and the dielectric, where d_j, $n_j + ik_j$, and θ_j are the layer thickness, the complex index of refraction, and the propagation angle for $MAPbI_3$ ($j = 1$) and dielectric ($j = 2$), respectively (see scheme of Figure 1c). The effect of the numerical aperture (*NA*) of the microscopic objective can be taken into account by averaging the incident angle from $\theta = 0$ to $\theta = \sin^{-1}(NA)$. From the angle-averaged reflectance we calculate numerically the tristimulus components:

$$\begin{aligned} X &= \int d\lambda P(\lambda) R(\lambda) x(\lambda), \\ Y &= \int d\lambda P(\lambda) R(\lambda) y(\lambda), \\ Z &= \int d\lambda P(\lambda) R(\lambda) z(\lambda), \end{aligned} \tag{2}$$

where $P(\lambda)$ is the power spectrum of the light source and $x(\lambda)$, $y(\lambda)$, and $z(\lambda)$ are the CIE color-matching functions. Finally, we convert eq 2 to the RGB color scheme using $(R,\ G,\ B)^T = (X,\ Y,\ Z)^T M^{-1}$, where the transformation matrix M depends on the white reference of the light source and other instrumental parameters.[22] Using the same method, and redefining the phase changes and the reflected amplitudes, we calculate also the RGB parameters, denoted R_0, G_0, and B_0, for dielectric/Si multilayer systems without $MAPbI_3$. Further details are given in the Supporting Information.

In Figure 2 we show the calculated perceived colors of $MAPbI_3$/dielectric/Si as a function of the $MAPbI_3$ and of the dielectric layer thicknesses, respectively d_1 and d_2, under an incident halogen light. In the calculations, we varied the thickness of the dielectric layer from $d_2 = 100$ nm to $d_2 = 500$ nm for the case of SiO_2, Figure 2a, and from $d_2 = 50$ nm to $d_2 = 300$ nm for TiO_2, Figure 2b. For all cases we have used the value $NA = 0.8$ for the numerical aperture of the microscope. From Figure 2a we see that, for a given SiO_2 thickness, the

calculated color of the multilayer changes distinctly with the thickness d_1 of $MAPbI_3$, at least for d_1 smaller than about 80 - 100 nm. Thicker $MAPbI_3$ films tend to have more saturated colors, with progressively less pronounced color variations as d_1 increases. A similar trend is observed for the $MAPbI_3/TiO_2/Si$ multilayers shown in Figure 2b. However, in this case color saturation sets in for somewhat smaller values of d_1 (about 50 - 70 nm), which is explained by the larger index of refraction n_2 of TiO_2 compared to that of SiO_2 (see Figure S2b in the Supporting Information). The difference between n_2 of TiO_2 and that of SiO_2 explains also that colors tend to saturate at thinner layers of TiO_2 compared to SiO_2.

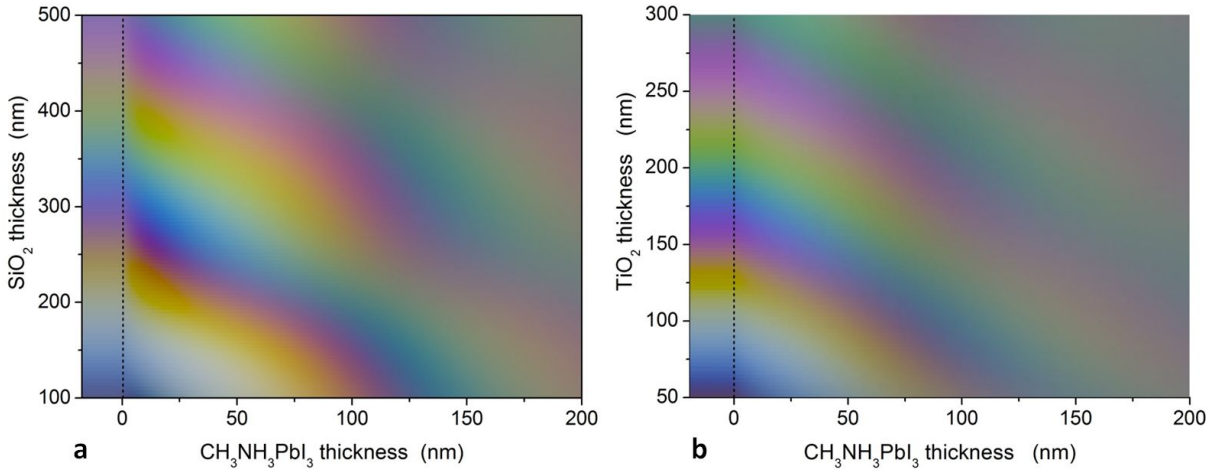

Figure 2. Calculated perceived colors of $MAPbI_3$/dielectric/Si multilayer system as a function of the perovskite thickness and of SiO_2 (a) and TiO_2 (b) thicknesses. The calculated colors shown on the left of the vertical dashed lines refer to dielectric/Si.

From the calculated colors for $d_2 = 280\,\text{nm}$ of Figure 2a, we see that the $MAPbI_3$ wires having blue color in Figure 1a are expected to have thicknesses in the range between ≈ 10 nm and $\approx 40\,\text{nm}$, while the orange portions of the wires should indicate thicknesses larger than about $50\,\text{nm}$. These estimates are in fair qualitative agreement with the thicknesses values

measured by AFM (Figure 1b), suggesting that the calculated color charts of Figure 2 may be exploited to characterize the size of $MAPbI_3$ wires.

3.2 RGB distance

Calculated color maps as those shown in Figure 2 are useful in establishing a qualitative or even semi-quantitative correspondence between film thicknesses and observed colors of multilayer systems. This correspondence can be set in more quantitative terms by calibrating the calculated colors with known thicknesses of the deposited material measured for example by AFM.[18,19] Here we introduce a one-step, calibration-free method that enables to reconstruct the film thickness directly from optical images. To this end, we measure the deviation from the experimental and calculated RGB parameter as follows. We denote $R^*(\vec{r})$, $G^*(\vec{r})$,and $B^*(\vec{r})$ the RGB components extracted at a given position $\vec{r}$ of an optical image of $MAPbI_3$/dielectric/Si, and R_0^*, G_0^*, and B_0^* the RGB components of the bilayer system dielectric/Si. Using the calculated and experimental RGB components we construct the vectors

$$\vec{v}(d_1)=\begin{bmatrix} R(d_1)/R_0 \\ G(d_1)/G_0 \\ B(d_1)/B_0 \end{bmatrix}, \quad \vec{v}^*(\vec{r})=\begin{bmatrix} R^*(\vec{r})/R_0^* \\ G^*(\vec{r})/G_0^* \\ B^*(\vec{r})/B_0^* \end{bmatrix} \tag{3}$$

from which we define the RGB distance as follows:

$$\Delta(\vec{r},d_1)=\left|\vec{v}(d_1)-\vec{v}^*(\vec{r})\right|. \tag{4}$$

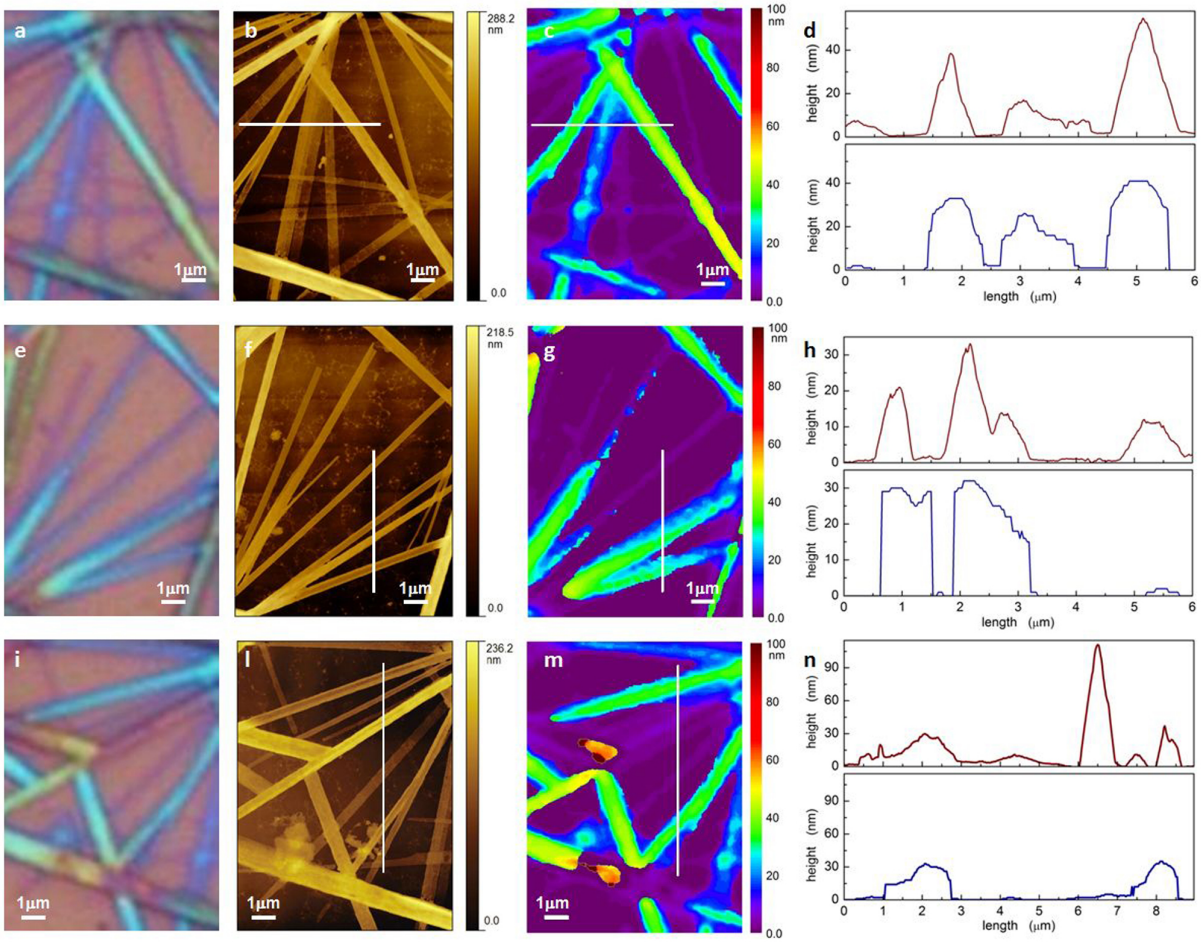

Figure 3. Optical (a,e,i) and AFM (b,f,l) micrographs of a set of nanowires extracted from Figure 1a,b. Reconstructed thickness maps obtained from the optical image are shown in panels (c,g,m). Panels (d,h,n) show profiles of the $MAPbI_3$ thickness obtained from AFM (upper panels) and from the reconstructed thickness maps (lower panels).

In the ideal situation in which calculated RGB parameters reproduce exactly the measured ones, the thickness d_1 for a given $\vec{r}$ would be given by the solution of $\Delta(\vec{r},d_1)=0$. There are however always some discrepancies between the calculated and measured RGB parameters, due to, for example, the non-perfect flat shapes of the nanowires, slight inhomogeneities of the dielectric thickness, and the approximated spectrum of the light source. We thus estimate the thickness of $MAPbI_3$ at a given position $\vec{r}$ of an optical image by finding the value of d_1 for which $\Delta(\vec{r},d_1)$ has an absolute minimum. Since the components of $\vec{v}(d_1)$ and $\vec{v}^*(\vec{r})$ are

measured with respected to the corresponding RGB values of the substrate, absolute minima of $\Delta(\vec{r},d_1)$ are expected to give a fair estimate of the actual wire thickness. From the color chart of Figure 2, we see that in principle this method is able to estimate $MAPbI_3$ thicknesses smaller than about $80-100$ nm for SiO_2/Si substrates and $50-70$ nm for TiO_2/Si substrates, which are the regions in Figure 2 where the calculated colors change more visibly with d_1.

3.3 Reconstruction of $MAPbI_3$ thicksesses

To reconstruct the wire thicknesses from optical images of $MAPbI_3$/dielectric/Si multilayers, we first calculate the RGB components (as described above) by increasing d_1 from 0 nm to 100 nm in steps of 1 nm, with dielectric thickness fixed at the measured value. Subsequently, for each pixel of the optical image we look for the value of d_1 such that $\Delta(\vec{r},d_1)$ is smallest. This process generally takes only a few seconds on a laptop computer even for images of about 1000×1000 pixels. We test this procedure on selected regions of the optical image of $MAPbI_3/SiO_2$/Si, shown in Figure 1a, by comparing the values of d_1 obtained from minimization of $\Delta(\vec{r},d_1)$ with the heights extracted from AFM measurements, as shown in Figure 3. From the d_1 maps shown in Figures 3c,g,m, and from the corresponding profiles reported in Figures 3d,h,n, we see that our method enables us to identify with overall good accuracy wire thicknesses comprised between 20 nm and 50 nm. Remarkably, even if the AFM profiles reveal that the upper surface of the wires is generally not perfectly flat, the reconstructed thicknesses are in good accord. The lower spatial resolution of the optical images compared to the AFM micrographs and the finite numerical aperture of the microscope contribute to round-off the fine details of the reconstructed thickness profiles. Furthermore, wires thickness smaller than about 15 nm are generally underestimated by the optical reconstruction, as seen by comparing the AFM profile of the first (last) peak of Figure

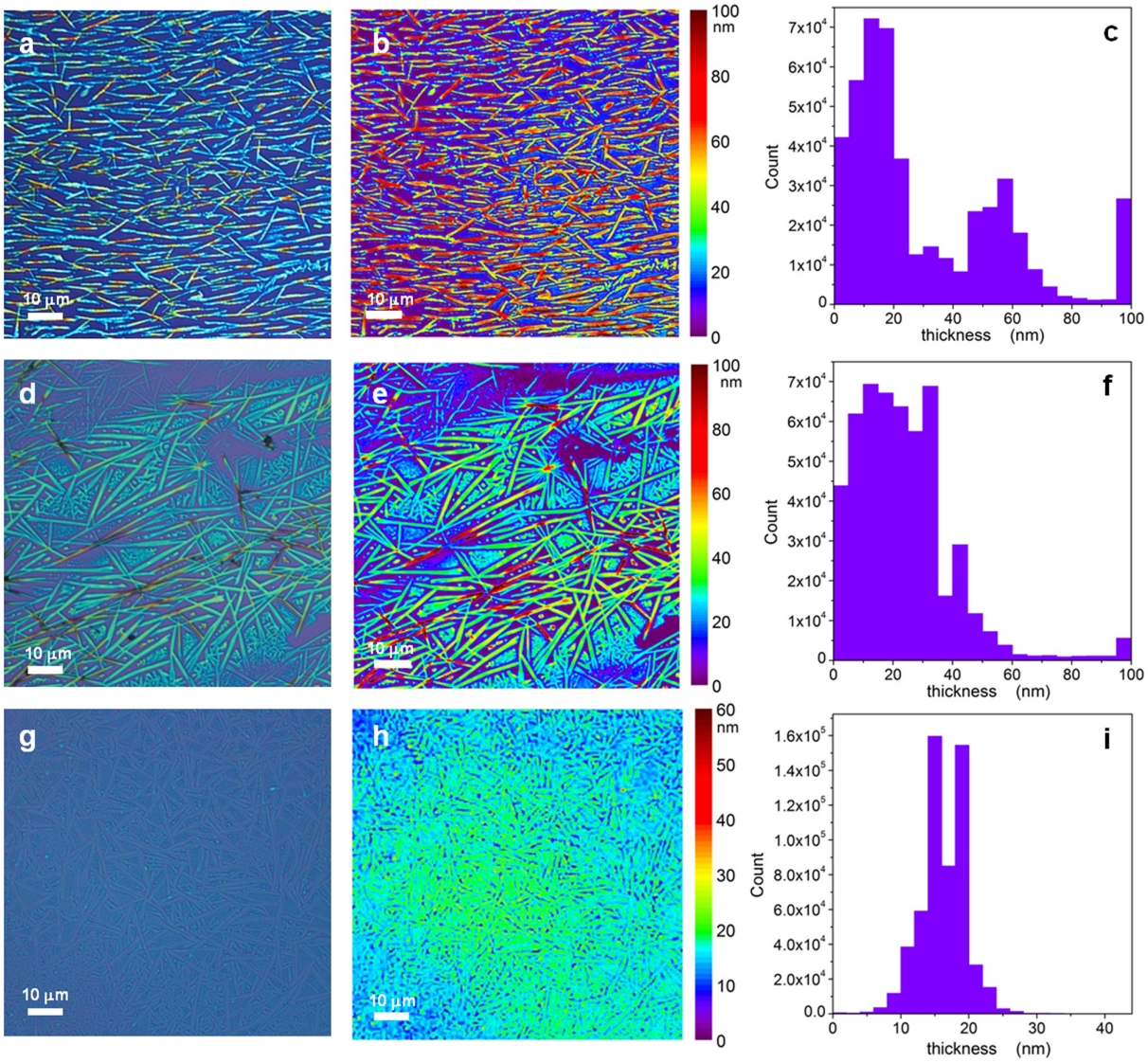

Figure 4. Optical micrographs (a,d,g), respective reconstructed thickness contrast maps (b,e,h), and extracted thickness distribution (c,f,i) for three different sets of nanowires slip-coated on two substrates with 100nm (top panels) and 500nm (middle and bottom panels) thick SiO_2.

3d (Figure 3h) with the corresponding profile of the reconstructed thickness. Note also that $MAPbI_3$ thicknesses greater than about 70 nm are not recognized, as evidence for example in Figure 3n, in which the peak of height ≈ 100 nm in the AFM profile is completely missing in the d_1 profile. By looking at optical image of Figure 3i, we see that the missing peak comes from a wire that has colors not much different from that of the SiO_2/Si substrate. We expect

thus that the use of different thicknesses of the SiO_2 layer would possibly increase the visibility of wires also thicker that 70 nm.

To assess the effect of the dielectric thickness and of the deposition process, we have reconstructed the wire thicknesses from optical images of $MAPbI_3$ slip-coated on SiO_2/Si substrates with $d_2 = 100$ nm and $d_2 = 500$ nm, as shown in Figure 4. From Figure 4c we see that the distribution of the reconstructed d_1 values for $d_2 = 100$ nm has a broad peak centered at $d_1 \approx 55$ nm with a tail extending above 80 nm. Note also that a portion of wires results to have thicknesses of about 100 nm or larger, as indicated by the peak at $d_1 \approx 100$ nm. A similar analysis of $MAPbI_3/SiO_2/Si$ with $d_2 = 500$ nm, shown in Figures 4d,e,f, suggests that the wires in this case have thicknesses broadly distributed up to about $d_1 \approx 60$ nm. The bottom panels of Figure 4 show our analysis for a dense film of $MAPbI_3$ nanowires slip-coated on 500 nm thick SiO_2 substrate: the reconstructed nanowire film thickness is narrowly distributed around approximately 15 nm, implying thus a fairly homogeneous coverage of the substrate. The results of Figure 4 show also that our method can automatically reconstruct thicknesses profiles from large-scale optical images, giving thus the possibility of performing statistical analyses as those presented in Figures 4c,f,i.

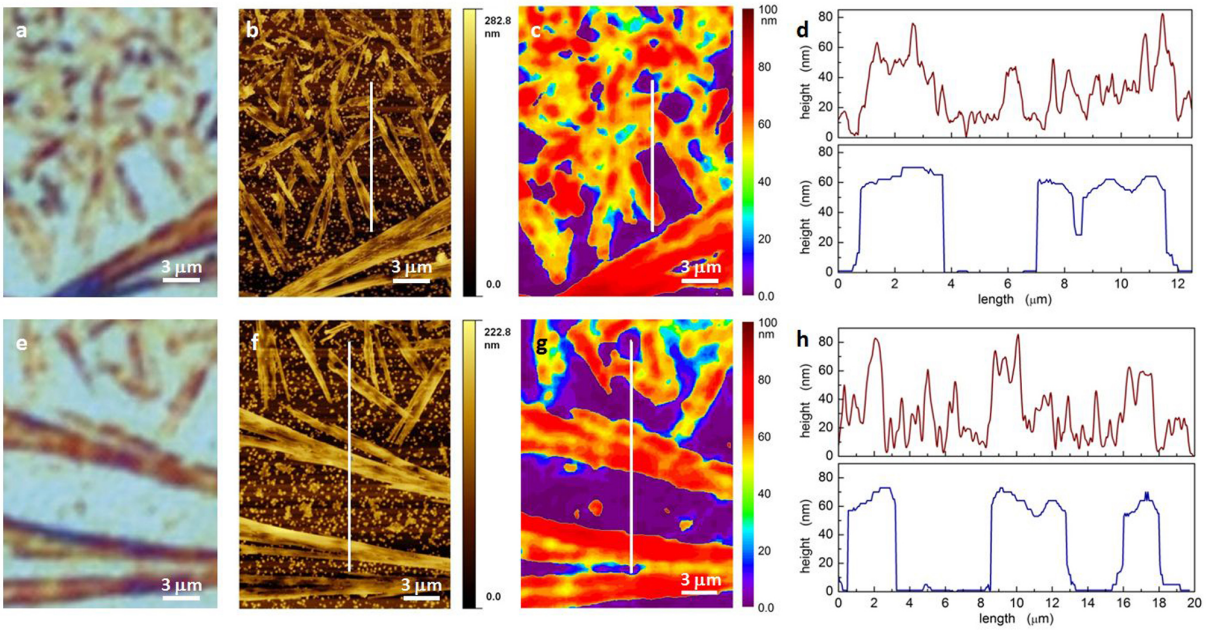

Figure 5. Optical (a,e) and AFM (b,f) micrographs of a set of nanowires slip-coated on TiO_2/Si substrate with d_2=100 nm. Reconstructed thickness maps obtained from the optical image are shown in panels (c,g). Figures (d,h) show profiles of the $MAPbI_3$ thickness obtained from AFM (upper panels) and from the reconstructed thickness maps (lower panels).

In Figure 5 we show the results of applying the minimization of $\Delta(\vec{r},d_1)$ to optical images of $MAPbI_3$ wires slip-coated on TiO_2/Si substrates with $d_2 = 100$ nm. Compared to the case with SiO_2/Si substrates, the AFM images (Figures 5b,f) reveal a substantial amount of $MAPbI_3$ nanoparticles deposited on the substrate. These nanoparticles are much less visible in Figures 5a,e due to the lower resolution of the optical imaging, and are thus largely not recognized by our method. Nevertheless, the reconstructed wire thicknesses shown in the maps and profiles of Figures 5c,g and Figures 5d,h, are in overall good accord with the heights measured by AFM. We note that the AFM profiles of $MAPbI_3/TiO_2$/Si display wire cross sections that are much more corrugated than those shown in Figure 3, with an average wire thickness which is however well captured by the reconstructed profiles shown in Figure 5d,h.

4 Conclusions

In conclusion, we have presented a method to easily read in a quick and quite reliable way the thickness of $MAPbI_3$ nanowires deposited on dielectric substrates directly from optical images in visible light. This approach takes advantage from the calculated color variation of $MAPbI_3$/dielectric/Si multilayers with the thickness of $MAPbI_3$ and correlates it with the observed colors. Minimization of a suitably defined RGB distance permits to calculate the values of the nanowire thickness which give the best agreement with the observed colors. Remarkably, this procedure does not involve calibration from other measurements (AFM, Raman) as it requires as only input optical images of the multilayer system. Comparison with AFM thickness profiles confirm that our method gives reliable and rapid estimates of the average $MAPbI_3$ thicknesses for different substrates. Nanowires up to about 80 nm in thickness can also be identified from large-scale optical images, permitting to determine the distribution of wire thicknesses for a given substrate. In principle, this method could be easily extended to automatically reconstruct thickness maps of other thin films or two-dimensional materials like, e.g., graphene and/or transition metal dichalcogenides, which thickness has been so far determined in a more indirect way through analysis of contrast[14,15,18,19] and color difference.[16,17]

ACKNOWLEDGEMENTS

M.S., B.N., L.F., and E.H. acknowledge financial support from the European Research Council through the Advanced ERC grant N° 670918 (Picoprop).

ASSOCIATED CONTENT

Supporting Information. Details on the calculation of the reflectance; refractive coefficients; CIE color matching functions; spectrum of halogen lamp; details on the conversion to the RGB components.

AUTHOR INFORMATION

Corresponding Author

*E-mail: claudio.grimaldi@epfl.ch. Tel.:+41-21-6934146

Notes

The authors declare no competing financial interest.

REFERENCES

[1] M. M Lee, J. Teuscher, T. Miyasaka, T. N. Murakami, H. J. Snaith, Science 2012, 338, 643.

[2] H.-S. Kim, C.-R. Lee, J.-H. Im, K.-B. Lee, T. Moehl, A. Marchioro, S.-J. Moon, R. Humphry-Baker, J. –H. Yum, J.-E. Moser, M. Grätzel, Sci. Rep. 2012, 2, 591.

[3] J. Burschka, N. Pellet, S.-J. Moon, R. Humphry-Baker, P. Gao, M. K. Nazeeruddin, M. Grätzel, Nature 2013, 499, 316.

[4] M. Liu, M. B. Johnston, H. J. Snaith, Nature 2013, 501, 395.

[5] N. J. Jeon, H. G. Lee, Y. C. Kim, J. Seo, J. H. Noh, J. Lee, S. I. Seok, J. Am. Chem. Soc. 2014, 136, 7837.

[6] N. J. Jeon, J. H. Noh, W. S. Yang, Y. C. Kim, S. Ryu, J. Seo, S. I. Seok, Nature 2015, 517, 476.

[7] National Renevable Energy Laboratory (NREL). Best Research-Cell Efficiencies, http://www.nrel.gov/ncpv/images/efficiency_chart.jpg (accessed: November 2015)

[8] G. Xing, N. Mathews, S. S. Lim, N. Yantara, X. Liu, D. Sabba, M. Grätzel, S.

Mhaisalkar, T. C. Sum, Nat. Mater. 2014, 13, 476.

[9] H. Zhu, Y. Fu, F. Meng, X. Wu, Z. Gong, Q. Ding, M. V. Gustafsson, M. T. Trinh, S. Jin, X.-Y. Zhu, Nat. Mater. 2015, 14, 636.

[10] Z.-K. Tan, R. S. Moghaddam, M. L. Lai, P. Docampo, R. Higler, F. Deschler, M. Price, A. Sadhanala, L. M. Pazos, D. Credgington, F. Hanusch, T. Bein, H. J. Snaith, R. H. Friend, Nat. Nanotechnol. 2014, 9, 687.http://www.nrel.gov/ncpv/images/efficiency_chart.jpg.

[11] M. Spina, M. Lehmann, B. Náfrádi, L. Bernard, E. Bonvin, R. Gaál, A. Magrez, L. Forró, E. Horváth, Small 2015, 11, 4824.

[12] D. Beaglehole, Rev. Sci. Instrum. 1988, 59, 2557.

[13] Q. Zhan, J. R. Leger, Appl. Opt. 2002, 41, 4443.

[14] I. Jung, M. Pelton, R. Piner, D. A. Dikin, S. Stankovich, S. Watcharotone, M. Hausner, R. S. Ruoff, Nano Lett. 2007, 7, 3569.

[15] P. Blake, E. W. Hill, A. H. Castro Neto, K. S. Novoselov, D. Jiang, R. Yang, T. J. Booth, A. K. Geim, Appl. Phys. Lett. 2007, 91, 063124.

[16] L. Gao, W. Ren, F. Li, H.-M. Cheng, ACS Nano 2008, 8, 1625.

[17] Y.-F. Chen, J. Phys. Chem. C 2011, 115, 6690.

[18] M. M. Benameur, B. Radisavljevic, J. S. Héron, S. Sahoo, H. Berger, A. Kis, Nanotechnology 2011, 22, 125706.

[19] H. Li, J. Wu, X. Huang, G. Lu, J. Yang, X. Lu, Q. Xiong, H. Zhang, ACS Nano 2013, 7, 10344.

[20] E. Horváth, M. Spina, Z. Szekrényes, K. Kamarás, R. Gall, D. Gacher, L. Forró, Nano Lett. 2014, 14, 6761.

[21] J.-H. Im, J. Luo, M. Franckevičius, N. Pellet, P. Gao, T. Moehl, S. M. Zakeeruddin, M. K. Nazeeruddin, M. Grätzel, N.-G. Park, Nano Lett. 2015, 15, 2120.

[22] J. Henrie, S. Kellis, S. M. Schultz, A. Hawkins, Opt. Express 2004, 12, 1464.

[23] H. A. Macleod, Thin-Film Optical Filters, Elsevier, New York 1969.